

Wavelength Dependence and Power Requirements of a Wavelength Converter Based on XPM in a Dispersion-Shifted Optical Fiber

Peter Öhlén, Bengt-Erik Olsson, and Daniel J. Blumenthal, *Member, IEEE*

Abstract—A 40-Gb/s wavelength converter based on cross-phase modulation in a dispersion-shifted fiber has been investigated through pulse measurements and simulation. The most important parameter is the dispersive walkoff, which makes the required input power wavelength dependent and determines the optical bandwidth. Simulations show the feasibility of the 160-Gb/s operation by using 2-ps pulses and a highly nonlinear dispersion-shifted fiber.

Index Terms—Cross-phase modulation, nonlinear fiber optics, optical fiber communication, optical networks, wavelength converters.

I. INTRODUCTION

ALL-OPTICAL wavelength conversion can play an important role in future ultrahigh-speed networks using wavelength-division multiplexing (WDM). The wavelength channels will probably be switched by optical add/drop multiplexers, optical crossconnects, and possibly optical packet switching techniques. Wavelength converters will greatly increase the flexibility in such networks and can be used as a basic switching element in, e.g., an optical crossconnect or an optical packet router [1].

Ultrahigh-speed wavelength conversion of return-to-zero (RZ) data has previously been demonstrated using four-wave mixing (FWM) in fiber [2] and semiconductor optical amplifiers [3] and by use of cross-phase modulation (XPM) in the nonlinear optical loop mirror [4]. Schemes using XPM and soliton formation [5] or XPM and polarization discrimination [6] have previously been proposed. We have recently demonstrated a different XPM-based scheme to wavelength convert 40-Gb/s RZ data [7].

The basic idea of this scheme is to utilize XPM in a dispersion shifted fiber. Continuous-wave (CW) light is launched into the fiber along with the data pulses. The pulses will impose a phase modulation that generates sidebands on the CW light. After suppression of the original CW wavelength, and filtering out one

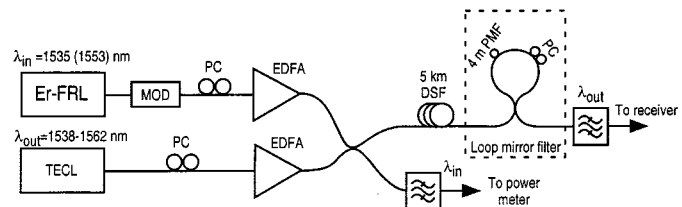


Fig. 1. Experimental setup of the XPM wavelength converter. Er-FRL: fiber ring laser; TECL: tunable external cavity laser; MOD: Mach-Zehnder modulator; EDFA: erbium-doped fiber amplifier; PC: polarization controller; PMF: polarization maintaining fiber; DSF: dispersion shifted fiber.

of the generated sidebands, the wavelength-converted data remain at the output. Here we report on pulse measurements in the wavelength converter in order to assess its fundamental operating characteristics at 40 Gb/s, as well as simulations using a highly nonlinear fiber and shorter pulses aiming at 160 Gb/s. For a wavelength converter, both the maximum data rate as well as the conversion wavelength span are important. When RZ data are used, it is important that the output pulsewidth is retained as well as having a stable operating point of the wavelength converter. When the wavelength changes, the optimum operating point will change, and the input power would have to be controlled to compensate for this. Together, these two effects will determine the optical bandwidth and the maximum bit rate of the wavelength converter.

II. EXPERIMENT

Fig. 1 shows the experimental setup where 8-ps pulses with a repetition rate of 10 GHz were generated from an actively mode-locked erbium-doped fiber ring laser, suitable for 40-Gb/s data. The pulses were gated with a Mach-Zehnder modulator to increase the available optical peak power, combined with CW light from a tunable external-cavity laser, and sent through 5 km of dispersion-shifted fiber with a zero-dispersion wavelength of 1542 nm. The pulse power was monitored at one port of the combiner. After the fiber, a loop-mirror filter (LMF) was used to notch out the original CW light, and a 0.4-nm band-pass filter was used to select one of the two generated sidebands. The loop-mirror filter has a sinusoidal filter function with repetitive notches, separated by 1 nm, and 27-dB suppression in the notches. An optically preamplified receiver with a 0.6-nm noise-suppression filter and a sampling oscilloscope was used to measure the pulse characteristics.

In the first experiment, pulses at 1535 nm were converted to longer wavelengths, and the CW light was varied from

Manuscript received December 20, 1999. This work was supported by the Defense Advanced Research Projects Agency under Center for Multidisciplinary Optical Switching Technology Grant F49620-96-1-0349 and under NGI Grant MDA972-99-1-0006.

P. Öhlén was with the Department of Electrical and Computer Engineering, University of California, Santa Barbara, CA 93106 USA. He is now with the Department of Electronics, Royal Institute of Technology, Kista S-164 40, Sweden.

B.-E. Olsson and D. J. Blumenthal are with the Department of Electrical and Computer Engineering, University of California, Santa Barbara, CA 93106 USA.

Publisher Item Identifier S 1041-1135(00)03599-0.

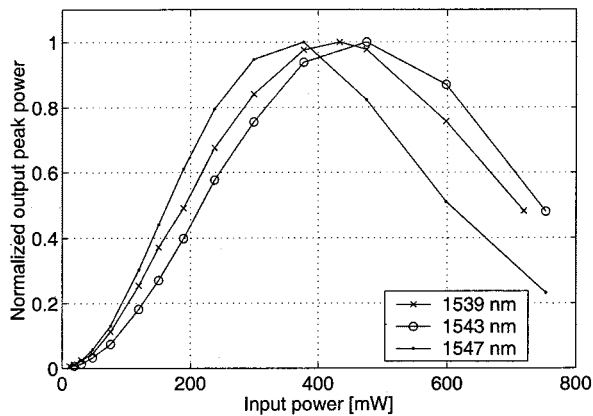


Fig. 2. Measured transfer functions for the wavelength converter using 8-ps input pulses and 5-km dispersion-shifted fiber.

1538 to 1558 nm. Depending on which sideband is chosen, the behavior is somewhat different. For the left sideband, the output pulsewidth of 12 ps is essentially transform limited over this wavelength range and given by the optical filter bandwidth. The right sideband shows the same behavior up to 1550 nm where the pulsewidth starts to increase, due to asymmetric spectral broadening due to SPM. In terms of optical power, the measured input–output transfer function has a nonlinear shape shown in Fig. 2 for three different wavelengths. When the wavelength separation between the pump and the CW light increases, the input pulse power required for maximum output power increases due to dispersive walkoff between the input pulses and the CW light. The input pulse power is then distributed over a time slice of the CW light, which corresponds to this walkoff. The maximum of the transfer function is chosen as the operating point. It should be noted that the wavelength converter can be used with input powers below the maximum of the transfer function, but this is a good reference point for the measurements and would also to some extent absorb variations in the input power. As shown in Fig. 3(a), the required input power for maximum output power increases when the wavelength is changed from 1538 nm, the dispersion slope was $0.086 \text{ ps/nm}^2/\text{km}$, the nonlinear refractive index $n_2 = 2.8 \cdot 10^{-20} \text{ m}^2/\text{W}$, the effective area $60 \text{ } \mu\text{m}^2$, and the loss 0.4 dB/km . The simulated pulsewidths for the left sideband vary between 12 and 13.5 ps for wavelengths between 1538 and 1555 nm, and the right sideband has similar pulsewidths until 1550 nm where the pulsewidth starts increasing, which is the same behavior as seen in the experiment. The required input power to reach the maximum of the transmission function is shown in Fig. 4 and has a good agreement to the measurements in Fig. 3. By using a highly nonlinear fiber [10], it is possible to decrease the required pulse power, or to use a shorter fiber, where the dispersive walkoff would be less significant. Fig. 4 also shows results for simulations with a 350-m-long highly nonlinear fiber with $n_2 = 5.2 \cdot 10^{-20} \text{ m}^2/\text{W}$ and an effective area of $10.7 \text{ } \mu\text{m}^2$, with the same loss and dispersion characteristics as the 5-km DSF. It can be seen that the difference between the left and right sideband is negligible and that the required input power only changes slightly, due to less dispersive walkoff. For this case, the simulated pulsewidths change only slightly between

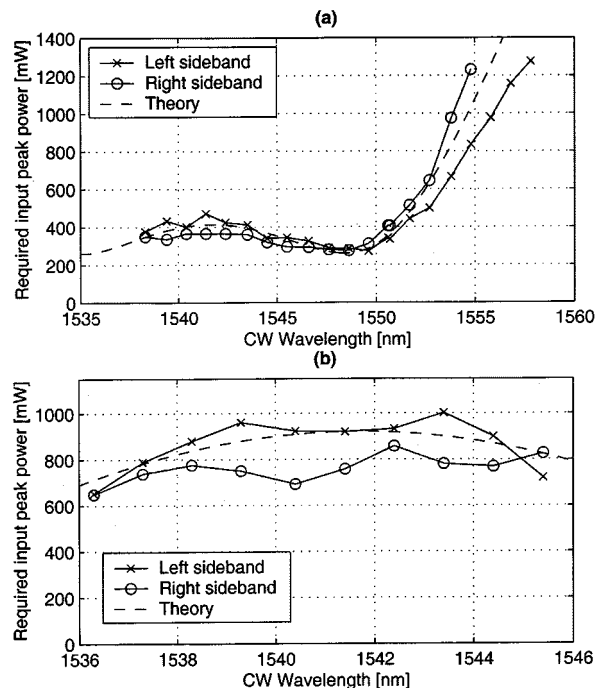


Fig. 3. Required input power to reach the maximum of the transfer function. Input pulses at (a) 1535 and (b) 1553 nm.

and higher order solitons will be generated. When the separation between the two wavelengths gets smaller, the spectrally broadened input pulses will interfere with the CW light, which generates interferometric noise in the output pulses. This effect starts to be significant at 1537 nm for input pulses at 1535 nm and at 1547 nm for input pulses at 1553 nm.

III. SIMULATION

The wavelength converter used in the experiment was simulated using the nonlinear Schrödinger equation and 8-ps unchirped Gaussian pulses. For the 5-km normal dispersion shifted fiber (DSF), the zero-dispersion wavelength was 1542 nm, the dispersion slope was $0.086 \text{ ps/nm}^2/\text{km}$, the nonlinear refractive index $n_2 = 2.8 \cdot 10^{-20} \text{ m}^2/\text{W}$, the effective area $60 \text{ } \mu\text{m}^2$, and the loss 0.4 dB/km . The simulated pulsewidths for the left sideband vary between 12 and 13.5 ps for wavelengths between 1538 and 1555 nm, and the right sideband has similar pulsewidths until 1550 nm where the pulsewidth starts increasing, which is the same behavior as seen in the experiment. The required input power to reach the maximum of the transmission function is shown in Fig. 4 and has a good agreement to the measurements in Fig. 3. By using a highly nonlinear fiber [10], it is possible to decrease the required pulse power, or to use a shorter fiber, where the dispersive walkoff would be less significant. Fig. 4 also shows results for simulations with a 350-m-long highly nonlinear fiber with $n_2 = 5.2 \cdot 10^{-20} \text{ m}^2/\text{W}$ and an effective area of $10.7 \text{ } \mu\text{m}^2$, with the same loss and dispersion characteristics as the 5-km DSF. It can be seen that the difference between the left and right sideband is negligible and that the required input power only changes slightly, due to less dispersive walkoff. For this case, the simulated pulsewidths change only slightly between

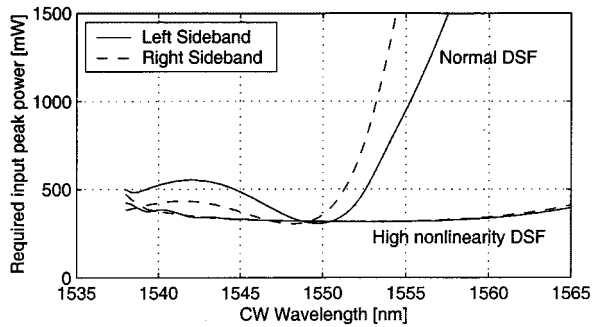


Fig. 4. Simulation of the wavelength converter using 8-ps input pulses at 1535 nm with 5-km normal DSF and 350-m highly nonlinear DSF.

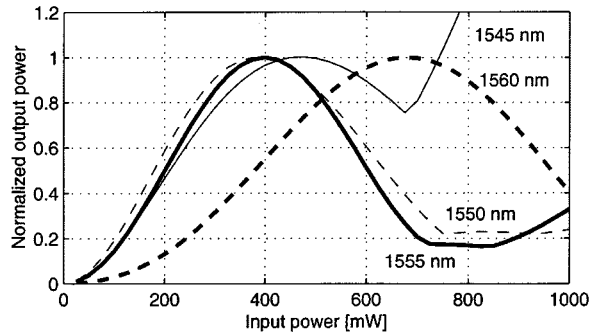


Fig. 5. Simulation of the transfer function for 2-ps input pulses at 1535 nm using a highly nonlinear DSF, aiming at 160 Gb/s.

12.1 and 12.5 ps for both sidebands. It would also be possible to use a 5-km-long highly nonlinear DSF, leading to the same behavior as the normal DSF, only that the required optical power would be decreased by a factor of ten.

Due to the fast response time of the fiber nonlinearity, it should be possible to use this wavelength converter at even higher speeds. To show this, a wavelength converter with 350-m highly nonlinear DSF was simulated with 2-ps input pulses, aiming at 160 Gb/s. The spacing of the LMF notches was 5 nm, and the bandpass filter has a 3-dB bandwidth of 1.8 nm. Fig. 5 shows the transfer function for four different wavelengths for 2-ps input pulses, using the left sideband. The rise in output power for the 1545-nm transfer function at 700-mW input peak power is due to the spectral broadening of the pump, which causes interferometric crosstalk on the new wavelength. Fig. 6 shows the required input peak power to reach the maximum of the transmission function with 350- and 35-m highly nonlinear DSF. The general behavior is similar to the 40-Gb/s case with standard DSF, where the required input power for the right sideband starts increasing before the left sideband for the long fiber. Also, the pulsewidth of the right sideband increases after 1550 nm, whereas the left sideband shows pulsewidths between 2.2 and 2.4 ps in the wavelength range 1544–1560 nm. For the 35-m fiber, the wavelength dependence is much smaller, but the required input powers are higher.

IV. CONCLUSION

We have investigated the wavelength dependence of a fiber-based 40-Gb/s wavelength converter and experimentally demonstrated a wavelength conversion span of 14 nm with a

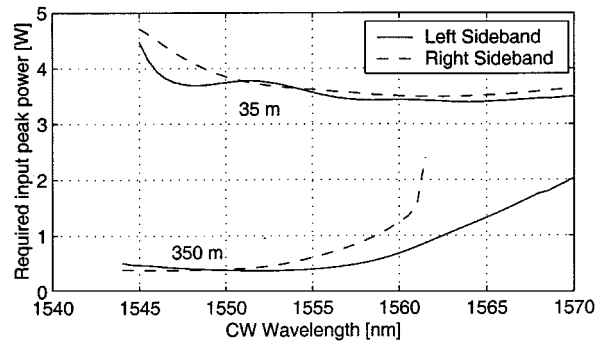


Fig. 6. Required input peak power to reach the maximum of the transfer function using 2-ps input pulses at 1535 nm using 350- and 35-m highly nonlinear dispersion-shifted fiber.

2-dB variation in the input power required for maximum output. In this range, the output pulsewidth was 12 ps. Simulations can reproduce the experimental results, and they show a substantial improvement if a highly nonlinear DSF could be used [10]. For this fiber, the power and pulse-width changes are very small over a wavelength range of over 20 nm, due to a much lower dispersive walkoff. This type of wavelength converter has a polarization dependence originating from the underlying XPM process. However, it can probably be made polarization independent by use of polarization scrambling in the dispersion shifted fiber [8] or circularly birefringent fiber [9]. Simulations with 2-ps pulses show that the scheme is probably scalable to even higher bit rates.

REFERENCES

- [1] B.-E. Olsson, P. Öhlén, L. Rau, G. Rossi, O. Jerphagnon, R. Doshi, D. S. Humphries, D. J. Blumenthal, V. Kaman, and J. E. Bowers, "Wavelength routing of 40 Gbit/s packets with 2.5 Gbit/s header erasure/rewriting using an all-fiber wavelength converter," in *Proc. ECOC'99*, Nice, France, postdeadline paper.
- [2] K. Inoue and H. Toba, "Wavelength conversion experiment using fiber four-wave mixing," *IEEE Photon. Technol. Lett.*, vol. 4, pp. 69–72, 1992.
- [3] S. Murata, A. Tomita, J. Shimizu, and A. Suzuki, "THz optical-frequency conversion of 1 Gb/s-signals using highly nondegenerate four-wave mixing in an InGaAsP semiconductor laser," *IEEE Photon. Technol. Lett.*, vol. 3, pp. 1021–1023, 1991.
- [4] K. A. Rauschenbach, K. L. Hall, J. C. Livas, and G. Raybon, "All-optical pulse width and wavelength conversion at 10 Gb/s using a nonlinear optical loop mirror," *IEEE Photon. Technol. Lett.*, vol. 6, pp. 1130–1132, 1994.
- [5] D. Schadt and B. Jaskorzynska, "Generation of short pulses from CW light by influence of crossphase modulation (CPM) in optical fibres," *Electron. Lett.*, vol. 23, pp. 1090–1091, 1987.
- [6] D. M. Patrick and A. D. Ellis, "10 GHz pulse train derived from a CW DFB laser using crossphase modulation in an optical fiber," *Electron. Lett.*, vol. 29, pp. 1391–1399, 1993.
- [7] B.-E. Olsson, P. Öhlén, L. Rau, and D. J. Blumenthal, "A simple and robust high-speed wavelength converter using fiber cross-phase modulation and filtering," in *Proc. Optical Fiber Communications Conf. (OFC'2000)*, Baltimore, MD, 2000, paper WE1.
- [8] B.-E. Olsson and P. A. Andrekson, "Polarization independent all-optical AND-gate using randomly birefringent fiber in a nonlinear optical loop mirror," in *Proc. Optical Fiber Communications Conf. (OFC'98)*, vol. 2, 1998, pp. 375–376.
- [9] Y. Liang, J. W. Lou, J. K. Andersen, J. C. Stocker, O. Boyraz, and M. N. Islam, "Polarization-insensitive nonlinear optical loop mirror demultiplexing with twisted fiber," *Opt. Lett.*, vol. 24, pp. 726–728, 1999.
- [10] M. Onishi, T. Okuno, T. Kashiwada, S. Ishikawa, N. Akasaka, and M. Nishimura, "Highly nonlinear dispersion-shifted fibers and their application to broadband wavelength converter," *Opt. Fiber Technol.*, vol. 4, pp. 204–214, 1998.